Korean J. Chem. Eng., **15**(4), 396-403 (1998)

EFFECT OF PRESSURE DROP ON PERFORMANCE OF HOLLOW-FIBER MEMBRANE MODULE FOR GAS PERMEATION

Daejun Chang†, Joonho Min, Sehern Oh and Kiho Moon

Hyundai Industrial Research Institute of Hyundai Heavy Industries,
Cheônha-dong 1, Dong-gu, Ulsan 682-792, South Korea
(Received 19 January 1998 • accepted 5 June 1998)

Abstract – The pressure drop mainly due to viscous friction inside hollow fibers is taken into consideration by nondimensionalization and numerical simulation of governing equations. For pure gas, the permeation pressure and velocity of actual situations with a viscous fluid deviate significantly from those of the corresponding inviscid or no-pressure-drop cases. The apparent permeability estimated from the relation of permeate flow rate and pressure difference is considerably underestimated in actual situations, and more severely for the region of small pressure difference and large module length. Numerical simulation shows that the estimated permeability behaves as if it were an increasing function of pressure difference for a constant permeability and roughly a constant for a dual-sorption-type permeability, respectively. For binary-mixture permeation the cut ratio and purity of permeate stream are mainly governed by two dimensionless parameters standing for pressure drop and permeability, respectively. The cut ratio and corresponding product composition are predictable without the rigorous simulation of the governing equations.

Key words: Pressure Drop, Numerical Simulation, Permeability Estimation, Dual-Sorption Model

INTRODUCTION

The estimation of permeability of individual components in a short module is one of the most basic objectives before the module is commercially applied to separation and purification of gaseous mixtures. Though plasticization, hydrostatic compression, and competitive sorption cause a deviation of permeability of a component in mixtures [Yi-Yan et al., 1980; Sanders and Koros, 1986; Thorman and Hwang, 1978], the estimation of permeability of a pure component is inevitable for further study on permeation of mixtures as well as for scale-up aiming at commercial applications.

The separation effectiveness of a commercial application of a hollow-fiber membrane to gas separation is commonly deteriorated by the pressure drop in the axial direction due to viscous friction, which is negligible for short modules [Antonson et al., 1977; Chern et al., 1985; Sidhoum et al., 1988; Kim et al., 1994]. In order to reduce the pressure drop, a mixture stream is usually fed into the shell side, and a part of it permeates through the membrane into the tube side. Even in these cases, the pressure drop in the tube side is considerable. Antonson et al. [1977] investigated the effects of design parameters, operating variables, flow patterns, and broken fibers on the separation performance. A similar approach was carried out by Chern et al. [1985] who showed axial pressure and velocity variations depending on inner diameter of fiber, feed pressure, feed composition, etc.

In spite of numerous investigations partially and entirely concerned with numerical study on a hollow-fiber module, how precisely the pure-gas permeability is estimated or how much the separation efficiency is deteriorated are not fully known. In the present study the pressure drop of commercial modules will be analyzed through numerical simulation. First, a set of governing equations will be introduced, which are based on constitutive relations and principal laws. Typical behaviors of pressure and velocity for inviscid and viscous fluids will be discussed. Then, the problems with parameter estimation for the permeability of a dual-sorption model will be revealed. Finally, the effect of pressure drop on cut ratio and product purity in binary mixtures will be considered.

†To whom all correspondence should be addressed.
E-mail: djchang@sbr.net

MATHEMATICAL DESCRIPTION AND SIMULATION

Consider a hollow-fiber module in which the retentate and permeate streams flow countercurrently. Neglecting radial dependence, diffusion, end-effects, physical deformation, and viscosity change, and assuming pressure drop to be described by the Hagen-Poiseuille equation, the pressure drop in the tube side is expressed by the equation [Antonson et al., 1977; Hwang and Kammermeyer, 1984; Sengupta and Sirkar, 1995; Kim and Lee, 1996].

$$\frac{dP^t}{dZ} = \frac{8\mu}{r_t^2} U^t \tag{1}$$

Similarly, the pressure drop in the shell side can be related to the velocity in the shell side by introducing a hydraulic or equivalent radius, r_s.

$$\frac{dP^s}{dZ} = -\frac{8\mu}{r_s^2} U^s \tag{2}$$

Note that the velocities are so defined as to be non-negative for countercurrent operation.

1. Pure-gas Permeation

For the control volume consisting of a hollow fiber and corresponding shell-side volume, the mass conservation for the column is expressed by following equations,

$$a_s \frac{dC^s U^s}{dZ} = -2\pi r_o J(r_o) \tag{3}$$

$$a_t \frac{dC^t U^t}{dZ} = -2\pi r_i J(r_i) \tag{4}$$

where the flux is given by the expression

$$J(r) = \frac{k(P^s, P^t)}{r \ln(r_o/r_i)} (P^s - P^t), \tag{5}$$

with the transfer from shell side to tube side taken to be positive. Strictly speaking, the permeability is also dependent on the lower pressure or the tube-side pressure. In many cases, the dependence is negligible due to the small ratio of the tube-side pressure to the shell-side one. It is well known that for a pure gas its permeance, which is defined as permeability divided by membrane thickness, is represented by a dual-sorption model [Barrer et al., 1958; Koros and Paul, 1978; Kim and Hong, 1997].

$$k(P^s) = \kappa_0 \left(1 + \frac{f}{1 + bP^s}\right) (r_o - r_i) \tag{6}$$

Since parameters f and b are positive in most cases, the permeability is usually a decreasing function of shell-side pressure.

For a comparison with simulated results, the apparent permeability is defined by the expression:

$$k' = \frac{Q_p}{A \cdot \Delta P} (r_o - r_i) \tag{7}$$

The pressure difference should be so defined as to be easily measurable or deducible from actual operation data. The pressure of the shell side remains nearly constant along the axial direction, and measurement at a point is a good representative, though it is available at any position by placing a pressure gauge. Measurement of the pressure of the tube side in usual modules is available only at one end of the module at which hollow fibers are potted. Usually, back-pressure controllers placed in retentate and permeate exits manipulate the shell and tube side pressures, respectively. Hence, the pressure difference can be defined as follows.

$$\Delta P \equiv P_L^s - P_0^t \tag{8}$$

It should be kept in mind that the shell-side pressure remains rather constant in the axial direction, and tube-side pressure does not.

In dimensionless form, the governing equations are expressed as follows:

$$\frac{dp^t}{dz} = \delta_1 u^t \tag{9}$$

$$\frac{dp^s}{dz} = -\delta_2 u^s \tag{10}$$

$$\frac{dp^t u^t}{dz} = -\delta_3 (p^s - p^t) \tag{11}$$

$$\frac{dp^s u^s}{dz} = -\delta_4 (p^s - p^t), \tag{12}$$

where the dimensionless parameters are defined by design specifications and operating conditions.

$$\delta_1 = \frac{8 \mu U_0 L}{r_i^2 P_L^s} \tag{13}$$

$$\delta_2 = \delta_1 \frac{r_i^2}{r_s^2} \tag{14}$$

$$\delta_3 = \frac{2\pi k_1 RTL}{a^t U_0 \ln(r_o/r_i)} \tag{15}$$

$$\delta_4 = \delta_3 \frac{a^t}{a^s} \tag{16}$$

The equivalent shell side radius is far greater than the inner radius of the fiber, and δ_2 is practically zero. Parameters δ_3 and δ_4 are closely related in magnitude with each other since the tube side cross-sectional area is of the same order as that of the shell side. In consequence, four parameters δ_1, δ_3, P_r, and ξ determine the behavior of pressure drop and velocity change.

2. Binary-mixture Permeation

In a binary system, each component permeates the membrane with the driving force of partial pressure difference.

$$J_f(r) = \frac{k_f(P_f^s, P_s^s)}{r \ln(r_o/r_i)} (P^s x^s - P^t x^t) \tag{17}$$

$$J_s(r) = \frac{k_s(P_f^s, P_s^s)}{r \ln(r_o/r_i)} [P^s(1 - x^s) - P^t(1 - x^t)] \tag{18}$$

Note that x^s and x^t represent the mole fraction of the 'fast' component in the shell and tube sides, respectively. The permeability of one component is generally dependent on the partial pressure of the other component, and expressed by combined dual-sorption model or free-volume theory. Since the overall behavior of the system is dominated by the permeation of fast components, its permeability is chosen as the characteristic scale for permeability.

In addition to two equations for pressure drop, two total-mass-conservation and two component-mass-conservation equations complete a set of governing equations for binary-mixture permeation, as follows,

$$\frac{dp^t u^t}{dz} = -\delta_3 \{p^s x^s - p^t x^t + \alpha[p^s(1 - x^s) - p^t(1 - x^t)]\} \tag{19}$$

$$\frac{dp^s u^s}{dz} = -\delta_4 \{p^s x^s - p^t x^t + \alpha[p^s(1 - x^s) - p^t(1 - x^t)]\} \tag{20}$$

$$\frac{dp^s u^s x^s}{dz} = -\delta_3 \{p^s x^s - p^t x^t\} \tag{21}$$

$$\frac{dp^t u^t x^t}{dz} = -\delta_4 \alpha [p^s(1 - x^s) - p^t(1 - x^t)], \tag{22}$$

where α is the ratio of permeability of the slow component to

that of the fast one. In consequence, compared with the pure-gas permeation, the behavior of the state variables of a binary mixture is additionally affected by the ratio as well as feed composition.

3. Numerical Simulation

The countercurrent-mode separation is in nature a two-point boundary value problem. In order to solve the equations numerically, the finite difference method is employed. Since the mass conservation equations are nonlinear, the difference equations are solved by Newton's method. In order to analyze numerical errors, a numerically exact solution is obtained with number of grids equal to 100; and it is found that the mean deviation of a numerical solution from the exact one is less than 10^{-4} if the number of grids is greater than 20.

Geometrical features of a commercial module are taken for numerical simulation, as shown in Table 1. For cases in which pressure drop is neglected or the fluid is inviscid, the viscosity of the gas is simply set to be zero. The permeability remaining invariant with respect to pressure is expressed by supposing the dual-sorption constant f to vanish. When some of the representative values are changed, it will be clearly noticed by additional statements.

There are usually two ways to estimate the permeability of pure gases in a hollow-fiber module. In one way the feed flow rate is regulated by a mass flow rate controller, and a part of it permeates the membrane. The pressures of the retentate and permeate sides are fixed by back pressure controllers. In the other way all of the feed stream is forced to permeate the membrane, and the pressure difference is regulated by the feed flow rate. In this case the cut ratio is equal to unity. The second method is easier to manipulate and less subject to measurement errors because the molar flow rate of feed is equal to that of the permeate stream. Consequently, the latter method is taken as the simulated problem for pure-gas permeation though the numerical solution can handle both of the cases, and the boundary conditions are given by the equations.

Table 1. Representative values used for pure-gas simulation

Hollow fiber		
r_i	9.1×10^{-5} m	
r_o	1.97×10^{-4} m	
Module		
Inner diameter	0.15 m	
L	2.0 m	
Number of fiber	3.2×10^{5}	
Viscosity		
μ	1.5×10^{-5} Pa s	for viscous fluid
	0	for inviscid fluid
Pressure		
$P^s(1)$	10 atm	
$P^t(0)$	1 atm	
Permeability, $k=\kappa_0\,[1+f(1+bP)^{-1}](r_o-r_i)$		
κ_0	2.0×10^{-4} $cm^3(STP)/cm^2$ s cmHg	
f	0.5	for pressure-dependent permeability
	0.	for constant permeability
b	0.1 atm	

$$p^t(0)=p_r,\ u^t(1)=0,\ p^s(1)=1,\ u^s(1)=0 \tag{23}$$

The last condition represents the dead-end operation. Note that in this case the feed flow rate and then the entrance velocity, which is taken as the characteristic scale, are not known until the calculation is completed.

For permeation of mixtures the dead-end operation is meaningless, and the cut ratio is closely related with the purity of product streams: the smaller the cut, the higher the mole fraction of the fast component in the permeate stream. Normally, the pressure of each side is fixed at a constant value, and the feed flow is regulated to attain a desired cut ratio. It is assumed that the mole fraction of the fast component at the dead-end is determined from the ratio of its flux to the total one [Hwang and Kammermeyer, 1984]. Consequently, the boundary conditions are given as follows.

$$p^t(0)=p_r,\ u^t(1)=0,\ p^s(1)=1,\ u^s(0)=1$$

$$x^s(0)=x_o,\ \frac{x^t(1)}{1-x^t(1)}=\frac{k_f}{k_s}\,\frac{x^s(1)-p_r x^t(1)}{1-x^s(1)-p_r[1-x^t(1)]} \tag{24}$$

That is, if the entrance velocity is known and the characterizing parameters are fully determined.

In order for practical systems to be simulated the characteristics of membrane modules in industrial applications are taken as the representative for numerical simulation [UBE Industries Product Catalog, 1994]. The values of permeance for fast and slow components are roughly those of carbon dioxide and nitrogen in the membrane. The operating pressure is closely related to the required cut ratio, product purity, membrane modulus, etc. Most industrial membrane modules, however, operate under the applied pressure of tens of atmospheric pressure. Consequently, the shell-side and tube-side pressures are taken to be 10 atm and 1 atm as reference values. In order to analyze the sensitivity of state variable to δ_1 and δ_3, the viscosity and permeance of the fast component are assumed to vary up to three times of their reference values.

RESULTS AND DISCUSSION

Fig. 1 shows the variations of pressure and velocity in the axial direction for constant permeability with the condition given in Table 1. As mentioned previously, the shell side has a friction factor far less than the tube side, and its pressure remains relatively constant. In contrast, the tube-side pressure of the viscous fluid increases nearly up to 5 atm due to frictional drag, while that of the inviscid fluid remains constant. In both cases the velocities of the shell and tube sides decrease with axial position. For the inviscid case the velocities in both sides change linearly since the pressure difference, and consequently the mass flux, through membrane are constant. For the viscous case the pressure difference or the driving force decrease with axial position, and the velocity of tube side shows a steep increase in the front part.

The result indicates that the estimation of permeability from experiments with hollow-fiber modules may lead to erroneous consequences without the pressure drop being taken into account. Such underestimation of apparent permeability becomes remarkable with increasing the module length, as shown in

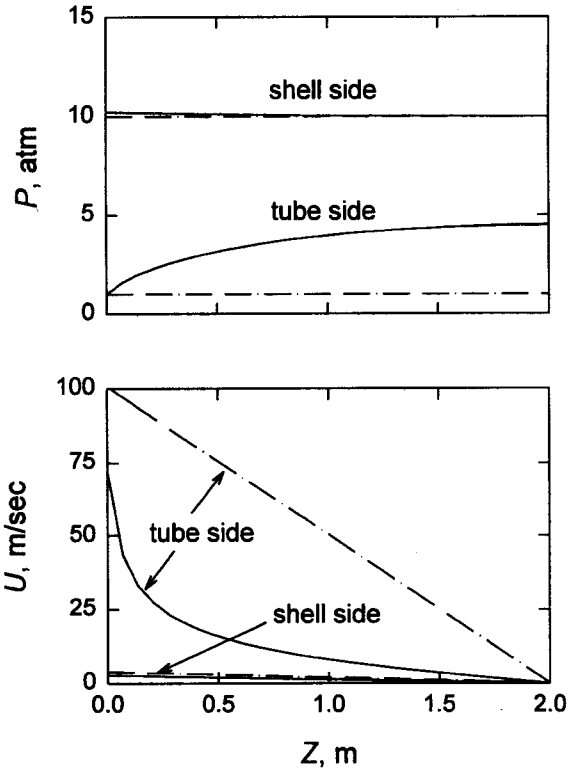

Fig. 1. Pressure and velocity variations in pure-gas permeation under the conditions given in Table 1. The dash-dot and solid curves correspond to inviscid and viscous fluids, respectively.

Fig. 2-(a), where all values except the module length are the same as in Table 1. The permeate flow rate of viscous flow is smaller than that of inviscid flow due to mitigated pressure difference. Such decrease in a flow rate results in the underestimation of apparent permeability, as depicted in Fig. 2-(a). For modules shorter than 0.2 m the underestimation is nearly negligible. The underestimation, however, becomes severe with module length. The result indicates that scale-up using modules with length equal to 1 m and 2 m may result in deteriorated performance by 10 % and 25 % decreases, respectively.

If the shell-side pressure is increased, the degree of underestimation becomes relieved, but the overall dependence of permeability on pressure is highly distorted, as presented in Fig. 2-(b). The permeate flow rate linearly increases with the applied pressure difference for the inviscid fluid, but not for the viscous case. The apparent permeability seems as if it were an increasing function of pressure with magnitude significantly underestimated. Note that for a high pressure, i.e., 100 atm, the difference of apparent permeability from the true one is still about 10 %. Following the previous discussion it is expected that the estimated permeability for the dual-sorption type should show a rather constant behavior with respect to pressure, and Fig. 2-(c) shows that is the case. Consequently, estimation of permeability from permeation experiments with hollow-fiber module would lead to results erroneous in overall trend with respect to pressure as well as in magnitude.

The results of estimation of permeability for constant and

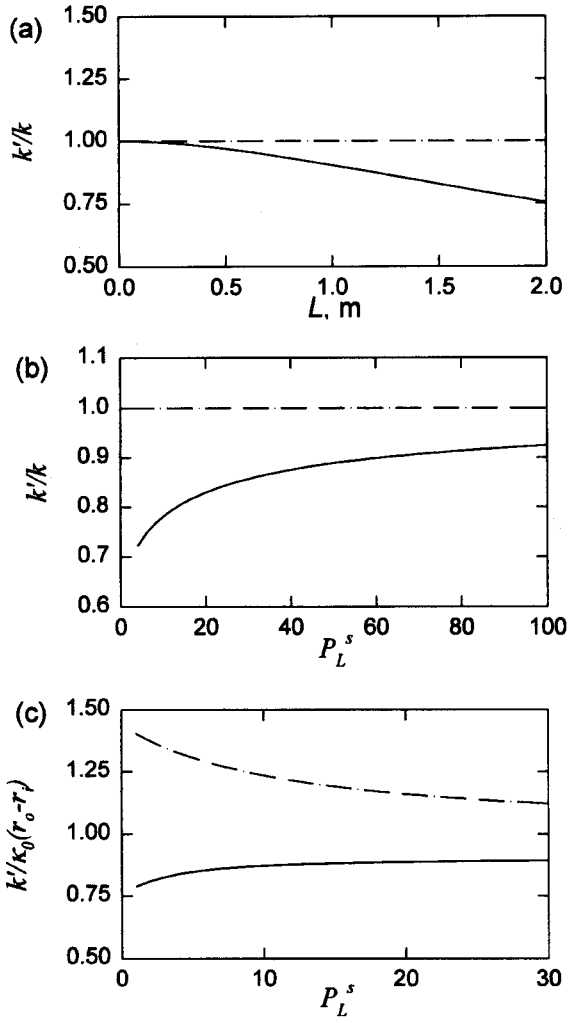

Fig. 2. Dependence of ratio of apparent permeability to asymptotic one: (a) on module length for constant permeability, (b) on shell-side pressure for constant permeability, and (c) on shell-side pressure for dual-sorption permeability. In each case the condition is given in Table 1 unless specified. The dash-dot and solid curves correspond to inviscid and viscous fluids, respectively.

dual-sorption models indicate that the permeability cannot be estimated accurately from the experimental results of hollow-fiber modules. For a constant permeability model the estimation gives a value significantly underestimated in magnitude. Usually, the dual-sorption parameters f and b are significantly sensitive, and a small scattering of measured data for flow rate causes significant deviations of estimated values. That is, a naive estimation leads the parameter b to take a negative value while its true value is non-negative. Since the pressure profile is not linear as shown in Fig. 1, the incorrect behavior cannot be overcome even if the pressure difference is defined such that $\Delta P \equiv [(P_L^s + P_0^s) - (P_L^t + P_0^t)]/2$. Such definition also overestimates the true pressure difference and underestimates the true permeability. The argument implies that the dual-sorption parameters estimated for commercial modules should likely be subject to large errors unless the effect of pressure drop is accounted for rigorously.

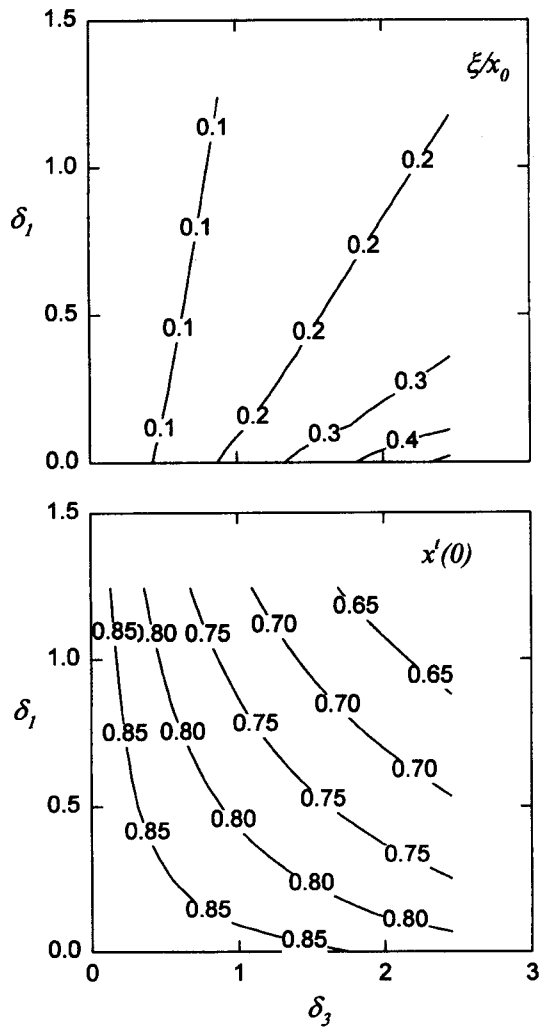

Fig. 3. Contour plot of cut ratio divided by feed mole fraction and mole fraction of permeate streams with respect to δ_1 and δ_3 with operating conditions given in Tables 1 and 2.

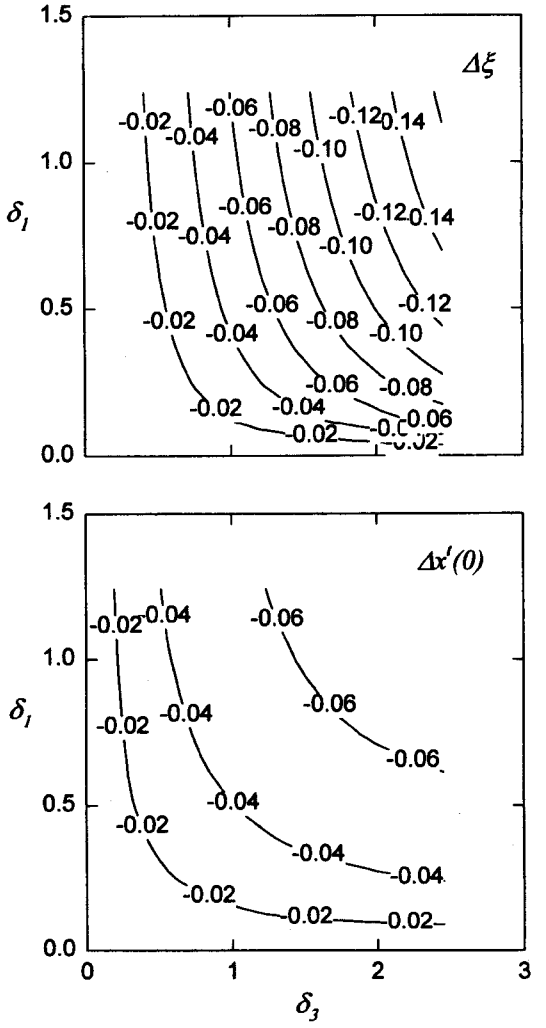

Fig. 4. Contour plot of deviation of cut ratio and mole fraction from those of inviscid fluid with operating conditions given in Tables 1 and 2.

In permeation systems for binary mixtures the productivity and purity are mainly governed by δ_1 and δ_3, which represent the relative pressure drop and permeability measures, respectively. Fig. 3 shows the variations of cut ratio divided by feed mole fraction and mole fraction of permeate stream with these parameters. Consistent with physical insight, for a constant δ_3 (or for a given module) the cut ratio decreases with δ_1 or with the fluid viscosity. The roughly equal spacing of neighboring iso-cut curves for inviscid cases (δ_1=0) suggests that the cut ratio for inviscid fluid is linearly proportional to δ_3 or to the relative permeability of penetrants through membrane. Since the iso-cut curves are nearly straight, such behavior preserves for non-zero δ_1 with the spacing increasing with δ_1.

The spacing between iso-cut curves for a constant δ_3, however, becomes large with δ_1. Similar behavior is also observed for the purity of permeate streams. Consequently, large δ_1 or considerable pressure drop causes the productivity and purity to decrease significantly. Fig. 4 shows how much the productivity and purity of viscous fluids are decreased due to the pressure drop effect. For small δ_3 or less permeable mem-

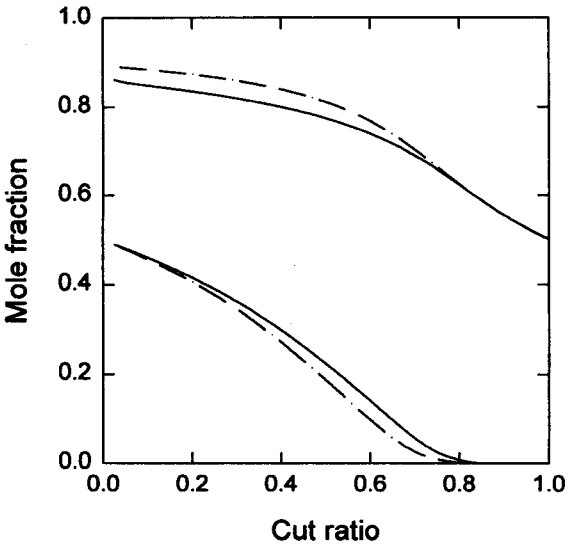

Fig. 5. Mole fraction of product streams with cut ratio for inviscid (dash-dot curves) and viscous (solid ones) fluids with conditions given in Tables 1 and 2.

brane the effect of pressure drop is nearly negligible. As δ_3 increases, the effect of δ_1 on both cut and purity becomes significant. The extents to which these decrease are not same. Fig. 5 shows the dependence of mole fraction in product streams on the cut ratio, with conditions given in Tables 1 and 2. At the same cut ratio the mole fraction in permeate stream decreases approximately by 0.02 for cut ratio less than a half. This decrease results in a corresponding increase of mole fraction in the retentate stream.

In commercial operation one of the major disturbances is the change of feed composition. Hence, it is important to anticipate the corresponding changes in cut ratio and mole fraction of the product stream. Fig. 6 shows results similar to those of Fig. 3 when the feed composition is raised to 0.7. Intrinsically, one can expect that the cut ratio and mole fraction of the fast component in permeate stream should increase. Comparison of Fig. 6 with Fig. 3 shows that the cut ratio divided by the feed composition remains relatively constant in spite of the change in the feed composition. The mole fraction of the fast component, however, is remarkably increased.

When the pressure ratio is small compared with unity, the variation of the permeating flux with the ratio is not considerable. Comparison of Fig. 3 with Fig. 7 where p_r is equal to 1/30 shows that the cut ratio and mole fraction remain relatively unchanged. The permeating flux is approximately proportional to $1-p_r$ in a dimensionless sense since the flux is scaled by the shell-side pressure. Hence, the ratio of permeating flux of Fig. 7 to that of Fig. 3 is in a rough sense proportional to (1–1/30)/(1–1/10). Consequently, the effect of pressure ratio on the cut-ratio is not significant unless it is

Table 2. Representative values used for simulation of binary-mixture permeation in addition to those given in Table 1

x_0	0.5
α	0.1
p_r	1/10
k_f	zero to three times of permeability in Table 1
μ	zero to three times of viscosity in Table 1

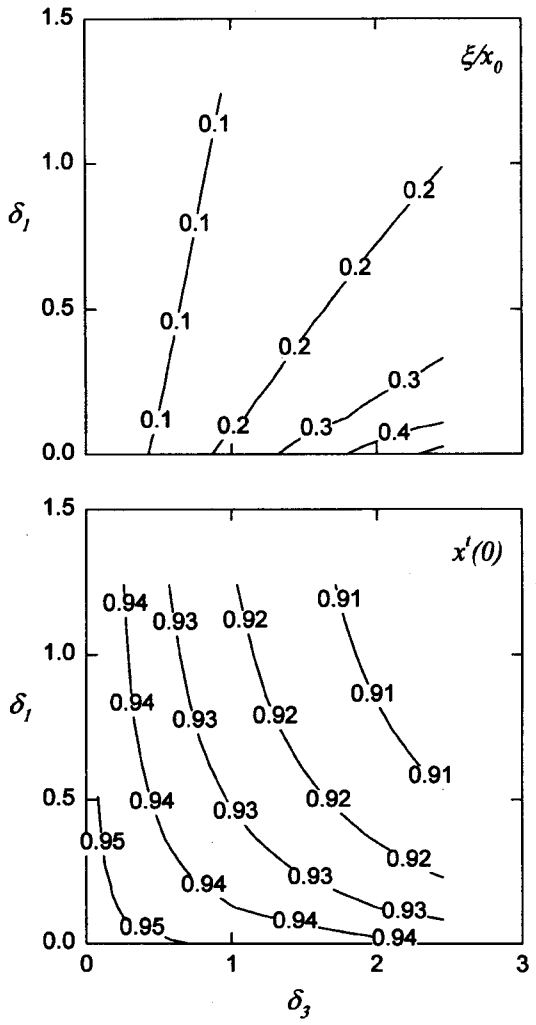

Fig. 6. Contour plot of cut ratio divided by feed mole fraction and mole fraction of permeate streams with respect to δ_1 and δ_3 with operating conditions given in Tables 1 and 2 except for x_0=0.7.

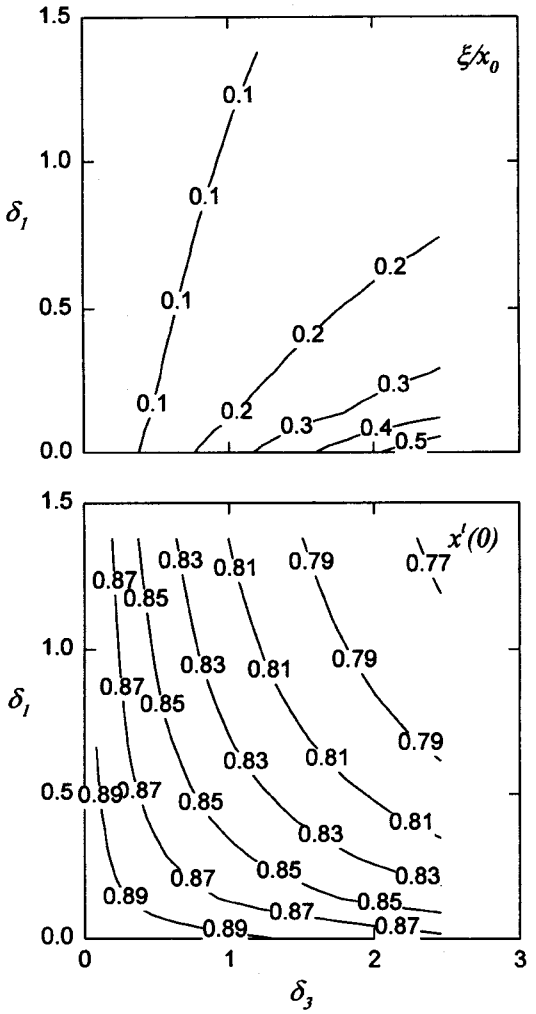

Fig. 7. Contour plot of cut ratio divided by feed mole fraction and mole fraction of permeate streams with respect to δ_1 and δ_3 with operating conditions given in Tables 1 and 2 except for p_r=1/30.

large enough to be comparable to unity.

Once an estimate of cut ratio is available, the corresponding composition of the product streams can be obtainable based on its relation with cut ratio such as shown in Fig. 4, which can be obtained with less effort. For example, consider the problem where the feed composition is changed with other operating conditions invariant. Then, one can estimate the new cut ratio based on the relation of ξ/x_0 remaining constant (note that Figs. 3 and 6 nearly overlap for cut ratio divided by feed composition). For the new feed composition, one can obtain a curve expressing the relation of the product composition and cut ratio by solving two ordinary differential equations rather than six. Finally, the new product composition can be revealed.

CONCLUSION

Simulation results for a hollow-fiber module, which is typically used in commercial applications, indicate that the apparent permeability may be underestimated unless the pressure drop or fluid viscosity is neglected. Such underestimation is more significant at lower pressure and in longer modules. Consequently, estimation of permeability from experiments with modules of commercial length may lead to permeability with magnitude being underestimated and dependence on pressure being distorted. Scale-up based on results from short modules may be subject to significant decrease in performance unless pressure drop is taken into consideration. For a given module, the precision can be improved by increasing the shell-side pressure. Such improvement of estimation precision is not significant due to the increases in velocity and consequently in the pressure drop in the tube side.

For permeation of a binary mixture, two parameters characterizing measures of the pressure drop and the permeability are introduced in terms of the design specifications and operating conditions. The effect of pressure drop on cut ratio as well as on purity of the fast component in permeating stream is considerable, especially for large δ_3 or for cases of highly permeable modules. The cut-ratio scaled by feed mole fraction, however, does not vary considerably. The purity of the fast component in permeate streams increases significantly with the feed mole fraction and pressure ratio. As operating conditions change, the cut ratio can be anticipated, and a rough estimate of the product composition can be obtainable based on the its relation to cut ratio.

NOMENCLATURE

A : total membrane area [m^2]
a : cross-sectional area [m^2]
b : constant for dual-sorption model [atm^{-1} or Pa^{-1}]
C : molar concentration [mol/m^3]
f : constant for dual-sorption model [dimensionless]
J : permeate flux [m^3(STP)/sec m^2]
k, k' : true and apparent permeability [cm^3(STP)cm/cm^2 s cmHg]
L : module length [m]
p, P : dimensionless and dimensional pressure [Pa]
P_r : ratio of the lower (tube-side) pressure to the higher (shell-side) one
Q_p : permeate flow rate [cm^3(STP)/s]
R : universal gas constant [8314 kg m^2/sec^2 kg-mole K]
r_i, r_o, r_s : inner and outer radii of a fiber, and equivalent radius of shell side [m]
u, U : dimensionless and dimensional velocity [m/sec]
x : mole fraction of the fast component
z, Z : dimensionless and dimensional axial coordinate [m]

Greek Letters

α : ratio of permeability of the slow to that of the fast
μ : gas viscosity [Pa sec]
$\delta_{1,2,3,4}$: dimensionless parameter
κ_0 : permeance [cm^3(STP)/cm^2 s cmHg]
ξ : cut ratio

Subscripts

f : for the fast component
s : for the slow component
0 : at z=0
L : at z=L

Superscripts

s : for shell-side component
t : for tube-side component

REFERENCES

Antonson, C. R., Gardner, R. J., King, C. F. and Ko, D. Y., "Analysis of Gas Separation by Permeation in Hollow Fibers", *Ind. Eng. Chem. Process Des. Dev.*, **16**, 463 (1977).

Barrer, R. M., Barrie, J. A. and Slater, J., "Sorption and Diffusion in Ethyl Cellulose and Rubber", *J. Polym. Sci.*, **27**, 177 (1958).

Chern, R. T., Koros, W. J. and Fedkiw, P. S., "Simulation of a Hollow-fiber Gas Separator: The Effects of Process and Design Variables", *Ind. Eng. Chem. Process Des. Dev.*, **24**, 1015 (1985).

Hwang, S.-T. and Kammermeyer, K., "Membranes in Separations", Robert E. Krieger Publishing Company, Malabar, 1984.

Kim, H.-J. and Hong, S.-I., "The Sorption and Permeation of CO_2 and CH_4 for Dimethylated Polysulfone Membrane", *Korean J. Chem. Eng.*, **3**, 14 (1997).

Kim, J.-S., Ahn, J.-S. and Lee, S.-M., "Separation Characteristics of CH_4-CO_2 Gas Mixture through Hollow Fiber Membrane Module", *Membrane J. (Korean)*, **4**, 197 (1994).

Kim, Y.-H. and Lee, E.-K., "Comparison of Axial and Radial Flow Chromatography on Protein Separation Speed and Resolution", *Korean J. Chem. Eng.*, **5**, 13 (1996).

Koros, W. J. and Paul, D. R., "Transient and Steady State Permeation in Poly(ethylene terephthalate) above and below Glass Transition", *J. Polym. Sci. Phys. Ed.*, **16**, 2171 (1978).

Sanders, E. S. and Koros, W. J., "Sorption of CO_2, C_2H_4, N_2O, and Their Binary Mixtures in Poly(methylmethacrylate)", *J. Polym. Sci., Polym. Phys. Ed.*, **24**, 175 (1986).

Sengupta, A. and Sirkar, K. K., "Analysis and Design of Membrane Permeators for Gas Separation", in Noble, R. D. and

Stern, S.A. (Ed.), Membrane Separations Technology. Principles and Applications, Elsevier, Amsterdam, pp. 499 (1995).

Sidhoum, M., Sengupta, A. and Sirkar, K.K., "Asymmetric Cellulose Acetate Hollow Fibers: Studies in Gas Permeation", *AIChE J.*, **34**, 417 (1988).

Thorman, J.M. and Hwang, S.-T., "Compressible Flow in Permeable Capillaries under Deformation", *Chem. Eng. Sci.*, **33**, 15 (1978).

Yi-Yan, N., Felder, R.M. and Koros, W.J., "Selective Permeation of Hydrocarbon Gases in Poly(tetrafluoroethylene) and Poly(fluoroethylene/propylene copolymer)", *J. Appl. Polym. Sci.*, **25**, 1755 (1980).

UBE Gas Separation System by Polyimide Membrane; UBE Industries Product Catalog, Tokyo, 1994.